

Occupancy-aware Trajectory Planning for Autonomous Valet Parking in Uncertain Dynamic Environments

Farhad Nawaz^{*1,2}, Faizan M. Tariq¹, Sangjae Bae¹, David Isele¹, Avinash Singh¹,
Nadia Figueroa², Nikolai Matni² and Jovin D'sa^{*1}

Abstract—Accurately reasoning about future parking spot availability and integrated planning is critical for enabling safe and efficient autonomous valet parking in dynamic, uncertain environments. Unlike existing methods that rely solely on instantaneous observations or static assumptions, we present an approach that predicts future parking spot occupancy by explicitly distinguishing between initially vacant and occupied spots, and by leveraging the predicted motion of dynamic agents. We introduce a probabilistic spot occupancy estimator that incorporates partial and noisy observations within a limited Field-of-View (FoV) model and accounts for the evolving uncertainty of unobserved regions. Coupled with this, we design a strategy planner that adaptively balances goal-directed parking maneuvers with exploratory navigation based on information gain, and intelligently incorporates wait-and-go behaviors at promising spots. Through randomized simulations emulating large parking lots, we demonstrate that our framework significantly improves parking efficiency, safety margins, and trajectory smoothness compared to existing approaches.

I. INTRODUCTION

In busy public spaces, parking consumes a lot of time, fuel and curb space, as drivers loop through parking lots searching for parking, interact with other drivers and pedestrians and perform tight maneuvers into a parking spot. Parking assistant systems that steer a car into a user-selected parking spot are now commercially available [1], [2], however a Type-1 autonomous valet parking system [3] that does not rely on infrastructure support is not yet available. We address the challenge of jointly selecting a parking spot and planning collision-free paths using only onboard sensor information.

Prior research in autonomous parking often has simplified assumptions that undermine realistic applicability. For instance, existing trajectory planners assume a predefined reference trajectory and focus only on static obstacle avoidance [4] or dynamic obstacle avoidance only for two-vehicle scenarios [5], neglecting the problem of identifying an optimal spot dynamically. Moreover, occupancy prediction methods traditionally rely on basic Bayesian filtering techniques without considering the influence of dynamic agents [6]. Their observation models assume constant sensor confidence irrespective of distance from the ego vehicle, disregarding the practical degradation of observation reliability with increased range. Additionally, exploration strategies in previous works [6], [7] overlook the downstream navigation task of executing the actual parking maneuver. In

particular, [7] employs a simplistic entropy-based model to represent spot occupancy distributions, limiting its ability for real-time decision-making under uncertainty. Furthermore, the frameworks in [8] assume complete observability of the parking environment, with full Vehicle-to-Vehicle (V2V) and Vehicle-to-Infrastructure (V2I) communication capabilities, and restrict themselves to offline spot assignment tasks without real-time strategic adjustments.

To address these gaps, we propose an occupancy-aware trajectory planning framework tailored for uncertain, dynamic parking scenarios with the following contributions:

- **Partial Observation model:** To consider partial observability, we introduce a shifted-rectangle Field-of-View model whose observation confidence decays with distance, thereby modeling the decreasing confidence of spots being available further away.
- **Spot Occupancy estimator:** We propose a Bayes filter based approach that predicts the future occupancy of parking spots using the behavior of dynamic agents in the scene. We also model distinct arrival and departure processes for initially vacant and initially occupied spots respectively, to reason about the future occupancy.
- **Strategy Planner:** We couple the occupancy beliefs with a cost-based policy that plans a trajectory for the ego to explore the lot or commit to a spot, balancing efficiency and safety.
- **Waiting for a spot:** We enable the ego vehicle to pause briefly near promising spots, capturing imminent vacancies that would otherwise be missed and reducing unnecessary exploration.

We evaluate our system in a simulated parking lot and show that our system reduces time and distance traveled to park and increases safety margins relative to existing methods, confirming that foresighted occupancy reasoning improves the overall valet parking performance.

II. PROBLEM FORMULATION AND APPROACH

We consider a parking lot environment, where the autonomous vehicle has prior access to the static map. The vehicle is equipped with onboard sensors that provide partial observations of parking spot occupancy within a limited FoV and also provides motion predictions of surrounding dynamic agents, such as vehicles and pedestrians. The task is to plan trajectories that guide the ego-vehicle to explore the parking lot, find an available parking spot, and park in a safe and efficient manner.

¹Honda Research Institute (HRI), San Jose, CA 95134, USA.

²GRASP Lab, University of Pennsylvania, PA 19104, USA.

*Corresponding authors: farhadn@seas.upenn.edu, jovin.dsa@honda-ri.com. All work was done when Farhad Nawaz was employed by HRI.

A. Parking Lot Environment

Consider the parking lot in Fig. 1 where there is a grid of N_p parking spots. The centers of all the spots in the lot are given by the set \mathcal{P} , where each $s_i \in \mathcal{P}$ is the two-dimensional Cartesian coordinates of the center of spot i , where $i \in \{1, 2, \dots, N_p\}$. We assume that the ego has prior access to the static map, which consists of the parking lot bounds, the centers of the spots \mathcal{P} and information about road lanes (center of road and lane width). The parking lot bounds are modeled as static obstacles as described in [9].

B. Vehicle Model

Let $x = (X, Y, \theta)$ be the state of the vehicle, where (X, Y) is the center of the rear axis and θ is the heading angle. We employ the kinematic bicycle model for vehicle dynamics which is well suited for vehicle at low speeds [10], given as

$$\dot{x} = f(x, u) \Leftrightarrow \begin{bmatrix} \dot{X} \\ \dot{Y} \\ \dot{\theta} \end{bmatrix} = \begin{bmatrix} v \cos(\theta) \\ v \sin(\theta) \\ \frac{v}{L} \tan(\delta) \end{bmatrix}. \quad (1)$$

The control input is $u = \begin{bmatrix} v \\ \delta \end{bmatrix}$, where v and δ is the longitudinal velocity and steering angle of the front wheel, respectively. The wheelbase of the vehicle is L , and the vehicle is modeled as a rectangle.

C. Observation Model

The limited on-board sensing capabilities is modeled using a FoV observation model based on a “scaled and shifted” infinity norm, with the sensing region biased towards the front of the vehicle.

Definition 1 (Distance metric). The scaled and shifted distance between the ego vehicle at state $x = [X \ Y \ \theta]^\top$ and a point $s \in \mathbb{R}^2$ is defined as

$$d_{(\zeta, r)}(x, s) = \left\| r^\top R(\theta)^\top \left(s - \left(\begin{bmatrix} X \\ Y \end{bmatrix} + R(\theta) \begin{bmatrix} \zeta \\ 0 \end{bmatrix} \right) \right) \right\|_\infty, \quad (2)$$

such that $r = \begin{bmatrix} \frac{1}{r_x} & \frac{1}{r_y} \end{bmatrix}^\top$, $R(\theta) = \begin{bmatrix} \cos(\theta) & -\sin(\theta) \\ \sin(\theta) & \cos(\theta) \end{bmatrix}$,

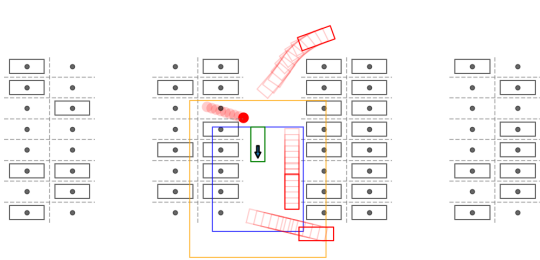


Fig. 1: Autonomous ego vehicle (green) with limited FoV (blue/orange) navigating a parking lot with dynamic vehicles (red rectangles) and a pedestrian (red circle). Spots are fully observed inside blue rectangle ($\epsilon = 1$), unobserved outside orange ($\gamma = 1.5$), and partially observed in between. Static vehicles are in black, and parking spot centers are grey dots.

where r_x and r_y define the half-lengths of the FoV rectangle along the longitudinal and lateral directions, respectively, while ζ is the forward shift in ego frame to bias the sensing region ahead of the vehicle. The rotation matrix $R(\theta)$ transforms vectors from the ego frame to the world frame.

Definition 2 (Spot observability). The *observability* of a spot $s \in \mathcal{P}$ from vehicle state x is defined as:

$$\text{Spot } s \text{ is } \begin{cases} \text{fully observed if} & d_{(\zeta, r)}(x, s) \leq \epsilon, \\ \text{unobserved if} & d_{(\zeta, r)}(x, s) \geq \gamma, \\ \text{partially observed} & \text{otherwise,} \end{cases} \quad (3)$$

where $\epsilon < \gamma$ and are obtained from the vehicle sensing limits.

The different observability regions are illustrated in Fig. 1.

Definition 3 (Observation accuracy). Let $O_t^s \in \{0, 1\}$ be the ground-truth occupancy and $Z_t^s \in \{0, 1\}$ be the observed occupancy of spot s at time t , where $1 := \text{occupied}$ and $0 := \text{vacant}$. The observation accuracy is modeled as the likelihood of correctly observing spot s using the below distance-dependent probability

$$\begin{aligned} p_c(d_{(\zeta, r)}(x, s)) &= P(Z_t^s = 1 | O_t^s = 1) = P(Z_t^s = 0 | O_t^s = 0), \\ p_c(d_{(\zeta, r)}(x, s)) &= e^{-\alpha \cdot \sigma(d_{(\zeta, r)}(x, s))} \text{ s.t. } \alpha, \\ \sigma(d_{(\zeta, r)}(x, s)) &= \frac{\ln(2)}{\alpha} \left(1 + e^{-\alpha_c(d_{(\zeta, r)}(x, s) - (\frac{\gamma - \epsilon}{2} + \epsilon))} \right)^{-1}. \end{aligned} \quad (4)$$

The function $\sigma(d)$ is a scaled sigmoid centered at $\frac{\gamma - \epsilon}{2} + \epsilon$ where $\alpha_c \gg 0$, with $\sigma(d) \approx 0$ when $d \approx \epsilon$ and $\sigma(d) \approx \frac{\ln(2)}{\alpha}$ when $d \approx \gamma$. Hence, $p_c(d) \rightarrow 1$ as $d \rightarrow \epsilon$ and $p_c(d) \rightarrow 0.5$ as $d \rightarrow \gamma$. Thus, our model captures how observation confidence decays with distance and varies by direction, unlike prior work [6] that assumes fixed uncertainty.

The formal problem statement is given below.

Problem 1. Given the state $x_t \in \mathbb{R}^3$ of the ego vehicle at time t , parking spot observations Z_t^s as defined in Section II-C, predictions of D dynamic agents $\{\{\hat{y}^j(k)\}_{k=t}^{t+T}\}_{j=1}^D$ over a horizon T , where $\hat{y}^j(k) \in \mathbb{R}^3$ is the position and heading of agent j if it is a vehicle, and $\hat{y}^j(k) \in \mathbb{R}^2$ is the position if agent j is a pedestrian; compute a sequence of control inputs $\{u_t, u_{t+1}, \dots, u_{t+T}\}$ for the kinematic model (1) that steers the vehicle to a feasible parking spot or explores the lot while avoiding both static obstacles and dynamic agents.

D. Proposed Approach

Fig. 2 illustrates our approach. At each planning step, we predict future parking spot occupancy over a horizon T using a recursive belief estimator that fuses our FoV observation model (Section II-C) with dynamic agent predictions. Our strategy planner then selects one of three actions—park immediately, wait near a potentially vacant spot, or explore the lot—by minimizing a cost balancing efficiency and safety. Hybrid A* is used in our path planner that generates a smooth, collision-free trajectory for execution, after which the loop repeats with updated observations.

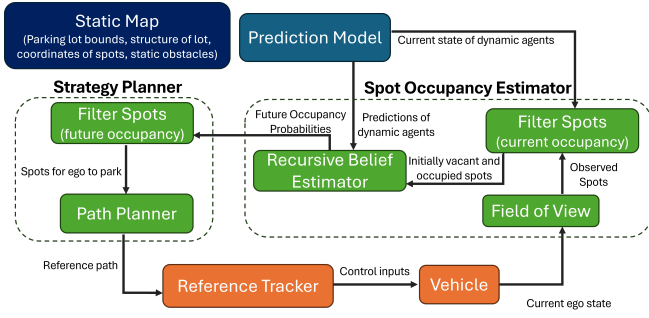


Fig. 2: Outline of our proposed approach.

III. SPOT OCCUPANCY ESTIMATOR

At each planning step t , the spot occupancy estimator predicts the probability of each parking spot being occupied over a horizon T , combining current sensor observations with the predicted trajectories of dynamic agents. This allows the ego vehicle to reason about which spots are vacant in the immediate future, guiding navigation based on anticipated occupancy rather than instantaneous observations.

We estimate parking spot occupancy probabilities using the Bayes Filter *predict* and *update* framework [11]. The prediction step models dynamic agents and their interactions with the environment, while the update step incorporates FoV observations as described in Section II-C.

A. Effect of Dynamic Agents

Each agent j 's predicted motion is modeled as a time-indexed Gaussian

$$y^j(k) \sim \mathcal{N}(\hat{y}^j(k), \Sigma(k)), \quad k \in \{t, \dots, t+T\}, \quad (5)$$

capturing both the nominal trajectory $\hat{y}^j(k)$ and increasing uncertainty over time. These uncertain trajectories are used to compute the probability that a parking spot $s \in \mathcal{P}$ is occupied by an agent j at time k :

$$p(s, j, k) = E_d \cdot A_f, \quad (6)$$

where the two terms in (6) are

$$E_d = ((\alpha_d + 1)(\alpha_d + e^{\alpha_1 m_d(y^j(k), s)}))^{-1}, \quad (7)$$

which is an exponential decay over the Mahalanobis distance [12] between the agent's position and the spot:

$$m_d(y^j(k), s) = (\hat{y}^j(k) - s)^T \Sigma(k)^{-1} (\hat{y}^j(k) - s),$$

and an alignment factor

$$A_f = \left(1 + e^{-\alpha_2 \sigma_v(k)^{-1} \hat{v}^j(k)^T (s - \hat{y}^j(k))}\right)^{-1} \quad (8)$$

capturing whether the agent is moving towards the spot, using the predicted velocity $\hat{v}^j(k)$ and velocity uncertainty $\sigma_v(k)$.

Uncertainty Propagation: We propagate the positional covariance at each timestep using the discrete-time model

$$\Sigma(k+1) = R(\theta(k)) (\Sigma(k) + Q) R(\theta(k))^T, \quad (9)$$

where $R(\theta(k))$ is the rotation matrix parameterized by the vehicle's heading $\theta(k)$ and Q is a diagonal matrix representing the process noise in ego frame. To estimate

the uncertainty in velocity, we use the finite difference $v^j(k) = \frac{y^j(k+1) - y^j(k)}{\Delta t}$ and (9).

From (6), the probability that at least one of the D dynamic agents will occupy spot s at time k is

$$q(s, k) = 1 - \prod_{j=1}^D (1 - p(s, j, k)). \quad (10)$$

At each future step $k \in \{t, \dots, t+T-1\}$, we predict the prior belief $\bar{b}_k^s = P(O_k^s = 1)$ based on the behavior of other agents, and update it using noisy, partial observations Z_k^s . The resulting posterior belief is $b_k^s = P(O_k^s = 1 | Z_k^s)$.

B. Prediction

In prior work [6], belief is propagated using a transition model that ignores interactions between dynamic agents and parking spots. In contrast, we explicitly incorporate dynamic agent predictions and model the asymmetry between spots that are initially vacant versus occupied. The initial state of a spot is determined from its observation Z_t^s under the FoV model in Section II-C. For spots outside the FoV, neither occupancy observations nor agent interactions are available.

- 1) For initially **vacant** spots, our transition model emphasizes incoming occupancy, and the prior belief is recursively updated as

$$\bar{b}_{k+1}^s = q(s, k+1)(1 - b_k^s) + \mu_1 b_k^s, \quad (11)$$

where $q(s, k+1) = P(O_{k+1}^s = 1 | O_k^s = 0)$ is computed from (10) and $\mu_1 = P(O_{k+1}^s = 1 | O_k^s = 1)$. The term μ_1 models the departure probability of a parked vehicle using an exponential distribution, reflecting the memory-less nature of departures. If λ_d denotes the average departure rate of a parked vehicle, the probability of departure within a time interval Δt is

$$P(O_{k+1}^s = 0 | O_k^s = 1) = 1 - e^{-\lambda_d \Delta t} \Rightarrow \mu_1 = e^{-\lambda_d \Delta t}. \quad (12)$$

- 2) For initially **occupied** spots, the emphasis is on potential departure of the occupied agent, captured as

$$1 - \bar{b}_{k+1}^s = \mu_2(1 - b_k^s) + (1 - q(s, k+1))b_k^s, \quad (13)$$

where $1 - q(s, k+1) = P(O_{k+1}^s = 0 | O_k^s = 1)$ is computed from (10) and $\mu_2 = P(O_{k+1}^s = 1 | O_k^s = 0)$. We model the arrival probability of a vacant spot using a Poisson distribution. If λ_a denotes the average number of vehicles that arrive with the time interval Δt , the probability that no vehicle parks in a vacant spot is

$$P(O_{k+1}^s = 0 | O_k^s = 0) = e^{-\lambda_a} \Rightarrow \mu_2 = 1 - e^{-\lambda_a}. \quad (14)$$

- 3) For **unobservable** spots, the prediction equation relies only on the average departure and arrival rates:

$$\bar{b}_{k+1}^s = \mu_2(1 - b_k^s) + \mu_1 b_k^s. \quad (15)$$

The predicted prior \bar{b}_{k+1}^s that is generated from the spot's occupancy history and dynamic agent predictions serves as the input for the update step to fuse the observations.

C. Update

The occupancy estimator combines current spot observations with predicted agent behaviors to estimate future occupancy, guiding ego vehicle navigation (Section IV). For fully observed spots, i.e., $p_c(d_{(\zeta,r)}(x_t, s)) = 1$, we fully trust the current observation and propagate occupancy using only agent predictions. For partially observed or unobserved spots, i.e., $p_c(d_{(\zeta,r)}(x_t, s)) < 1$, we apply Bayes' rule to fuse the observation with the prior belief as

$$b_{k+1}^s = \begin{cases} \bar{b}_{k+1}^s & \text{if } p_c(d_{(\zeta,r)}(x_t, s)) = 1 \\ \frac{P(Z_{k+1}^s | O_{k+1}^s = 1) \bar{b}_{k+1}^s}{P(Z_{k+1}^s)} & \text{otherwise,} \end{cases} \quad (16)$$

where x_t is the current state of the ego. Since only the current occupancy observation Z_t^s is available, we set $Z_{k+1}^s = Z_t^s$ for all $k \in \{t, \dots, t+T-1\}$. For all unobserved spots s , from (4), we have $p_c(d_{(\zeta,r)}(x_t, s)) \approx 0.5$. Hence, using (16), the update equation reduces to $b_{k+1}^s \approx \bar{b}_{k+1}^s$, i.e., the prior belief remains unchanged.

IV. STRATEGY PLANNER

The Strategy Planner leverages probabilistic occupancy forecasts from the Spot Occupancy Estimator to select actions such as parking, waiting, or exploring, and generates a reference trajectory that balances efficiency and safety in dynamic parking environments.

A. Promising Spots to Park

At each planning step, we filter candidate parking spots inside the FoV based on the occupancy predictions, classifying spots that are promising for the ego vehicle to park.

Spot s is vacant in the future ($t+T$) if

$$\begin{cases} s \text{ is } \mathbf{initially\ vacant} \text{ (time } t) \text{ and } b_{t+T}^s \leq P_v, \\ s \text{ is } \mathbf{initially\ occupied} \text{ (time } t) \text{ and } b_{t+T}^s \leq P_o. \end{cases} \quad (17)$$

We typically set $P_v < P_o$ reflecting the asymmetric reasoning for spot availability. An initially vacant spot must remain vacant with high probability—otherwise, it is likely to be claimed by another agent and thus unsuitable for the ego to park. In contrast, an initially occupied spot can be considered promising even with a lower probability of becoming vacant, as this indicates the occupying agent is likely to leave, creating an opportunity for the ego to park. This occupancy-based filtering ensures that the strategy planner only considers realistic and feasible parking spots, optimizing decision-making efficiency and safety in dynamic environments.

B. Compute and Evaluate Paths

If multiple spots are estimated to be vacant within the FoV by (17), we evaluate candidate paths and prioritize them using a cost function that promotes parking efficiency and smooth maneuvers. At planning step t , let $\mathcal{S}_t \subset \mathcal{P}$ be the set of spots classified as vacant via (17). From the ego state $x_t = [X_t, Y_t, \theta_t]^\top$, we compute paths $\mathcal{T} = \{\tau_g\}_{g \in \mathcal{S}_t}$, where each τ_g leads to a goal state g . We use Hybrid A star to generate paths that avoid the static obstacles, though alternative methods (e.g., sampling or spline-based

planners [13], [14]) may also be applied. Path computations are parallelized across all candidate spots g for efficiency.

1) *Cost function*: We evaluate which among $\{\tau_g\}_{g \in \mathcal{S}_t}$ is the optimal path for the ego vehicle to follow using a cost function. A path is defined as $\tau_g = \{x(k)\}_{k=t}^{t+N_g}$, where $x(t) = x_t$, $x(t+N_g) = g$ and N_g is the time required to reach the goal g from the current state x_t . We use the following cost function to prioritize the paths.

$$\mathcal{C}(\tau_g) = N_g + t_w + \sum_{k=t}^{t+t_w} c_o(x(k), \mathcal{Y}(k)) + \sum_{k=t+t_w+1}^{t+t_w+N_g} c_o(x(k-t_w), \mathcal{Y}(k)) + \sum_{k=t}^{t+N_g-1} c_{\text{smooth}}(x(k)), \quad (18)$$

where t_w denotes the *waiting time* which is explained later, $\mathcal{Y}(k) = \{\hat{y}^j(k)\}_{j=1}^D$ represents the configuration of dynamic agents at time k and the static obstacles are given by $\{w_i\}_{i=1}^W$, where $w_i \in \mathbb{R}^2$. The per-stage cost $c_o(\cdot, \cdot)$ penalizes proximity to obstacles, while $c_{\text{smooth}}(\cdot)$ promotes smooth trajectories, as defined below.

$$c_o(x(k), \mathcal{Y}(k)) = \sum_{j=1}^D h(x(k), \hat{y}^j(k)) + \sum_{i=1}^W h(x(k), w_i), \quad (19)$$

$$c_{\text{smooth}}(x(k)) = \|a(k)\| + \text{Dc}(v(k), v(k+1)) + \mathbb{1}(\text{reverse}(k)) + \mathbb{1}(\text{change_gear}(k)), \quad (20)$$

where $\text{Dc}(\cdot, \cdot)$ is the cosine distance between two vectors [15]. Other terms in the smoothness cost $c_{\text{smooth}}(\cdot)$ are

$$\begin{aligned} a(k) &= [\ddot{X}(k), \ddot{Y}(k)]^\top, \quad v(k) = [\dot{X}(k), \dot{Y}(k)]^\top, \\ \mathbb{1}(\text{reverse}(k)) &= \begin{cases} 1, & \text{if } \text{Dc}\left(v(k), \begin{bmatrix} \cos(\theta(k)) \\ \sin(\theta(k)) \end{bmatrix}\right) > 1, \\ 0, & \text{otherwise} \end{cases}, \\ \mathbb{1}(\text{change_gear}(k)) &= \begin{cases} 1, & \text{if } \text{Dc}(v(k), v(k+1)) > 1, \\ 0, & \text{otherwise.} \end{cases} \end{aligned} \quad (21)$$

The obstacle avoidance cost $h(\cdot, \cdot)$ is

$$h(x, y) = e^{-\alpha_o d_o(x, y)}, \quad (22)$$

$d_o(x, y)$ is the distance between the ego vehicle x and obstacle y . The barrier cost $h(\cdot, \cdot)$ penalizes proximity to obstacles, with $\alpha_o = 2$ for dynamic agents and $\alpha_o = 3$ for static ones, reflecting smaller penalties for static obstacles. We extend the 3-circle distance from [16] to a 5-circle model for $d_o(\cdot, \cdot)$ to improve accuracy for dynamic collision avoidance. For static obstacles, we instead compute the exact distance between the ego vehicle's edge and obstacle points $\{w_i\}_{i=1}^W$ [9], since static obstacle positions are more reliably perceived. To balance terms, $\|a(t)\|$ and the cosine distance are scaled to $[0, 1]$ using velocity limits, while $h(x, y) \in [0, 1]$ from (22).

2) *Waiting time*: We incorporate *wait and go* behaviors into the planned paths τ_g using the waiting time t_w in (18). This enables the ego vehicle to yield to dynamic agents and park in a spot g that is estimated to be vacant in the near future by our Spot Occupancy Estimator (Section III). To ensure feasibility, we impose a maximum wait time T_w and evaluate only paths with $t_w \leq T_w$.

Remark: If $T < N_g$, we extrapolate the predictions using a constant velocity model as $\hat{y}^j(k) = \int_{s=t+T}^k \hat{v}^j(t+T-1)ds$ for all $k \geq t+T+1$ and $j \in \{1, 2, \dots, D\}$, where $\hat{v}^j(k) = \frac{\hat{y}^j(k+1) - \hat{y}^j(k)}{\Delta t}$.

Once we compute the paths $\mathcal{T} = \{\tau_g\}_{g \in \mathcal{S}_t}$ and their associated costs $\mathcal{C}(\tau_g)$, we choose the path that has the minimum cost $\arg \min_{\tau \in \mathcal{T}} \mathcal{C}(\tau)$ and avoids all the obstacles respecting the safety thresholds. We set larger safety thresholds for dynamic agents—50 cm for vehicles and 90 cm for pedestrians—compared to 20 cm for static obstacles.

C. Exploration

If no feasible path exists to a spot in \mathcal{S}_t , the ego vehicle switches to exploratory mode, selecting a path that maximizes information gain about spot occupancy. In typical parking lots such as Fig. 1, maneuver options are limited: continuing straight within a row, entering a row from outside, and turning left or right at its end. We generalize this decision-making process by evaluating paths to a finite set of exploration goals $\mathcal{E} \subset \mathbb{R}^3$, where each $e \in \mathcal{E}$ denotes a candidate goal pose.

1) *Exploration goals*: We define three exploration goals $\mathcal{E} = \{e_1, e_2, e_3\}$ at each time step: going straight (e_1), turning left (e_2), and turning right (e_3). These options suit structured parking lots with parallel rows (Fig. 1), though we plan to extend them to more general layouts such as multi-level garages in future work. The straight goal is

$$e_1 = \begin{bmatrix} R(\theta_t) \begin{bmatrix} \epsilon - \eta \\ 0 \end{bmatrix} + \begin{bmatrix} X_t \\ Y_t \end{bmatrix} \\ \theta_t \end{bmatrix}, \quad (23)$$

where $x_t = [X_t, Y_t, \theta_t]^\top$ is the ego state, ϵ is the full observability threshold (Sec. II-C), and $0 \leq \eta < \epsilon$ denotes how far the ego moves forward.

Left and right turn goals are

$$\begin{aligned} e_2 &= \begin{bmatrix} R(\theta_t) \begin{bmatrix} x_{\text{road}} + \frac{l_w}{2} \\ \epsilon \end{bmatrix} + \begin{bmatrix} X_t \\ Y_t \end{bmatrix} \\ \theta_t + \frac{\pi}{2} \end{bmatrix}, \\ e_3 &= \begin{bmatrix} R(\theta_t) \begin{bmatrix} x_{\text{road}} - \frac{l_w}{2} \\ -\epsilon \end{bmatrix} + \begin{bmatrix} X_t \\ Y_t \end{bmatrix} \\ \theta_t - \frac{\pi}{2} \end{bmatrix}, \end{aligned} \quad (24)$$

where x_{road} is the center of the newly observed road, and l_w its lane width. The offsets $\pm \frac{l_w}{2}$ encode left and right turns under right-hand traffic convention, with corresponding adjustments to heading and y -coordinate sign.

2) *Information gain*: We generate paths to the exploration goals using Hybrid A star for e_2 and e_3 , and a 5th-order spline to interpolate a path from the current state x_t to e_1 . Let $\mathcal{T}' = \{\tau_e\}_{e \in \mathcal{E}}$ denote the set of paths from x_t to each goal. To evaluate the information gain of a path, we consider the entropy of a parking spot s at time k as

$$\mathcal{H}(b_k^s) = -b_k^s \log_2(b_k^s) - (1 - b_k^s) \log_2(1 - b_k^s), \quad (25)$$

where $b_k^s = P(O_k^s = 1 | Z_k^s)$ is the probability that spot s is occupied given observation Z_k^s . We simulate future observations $\{Z_k^s\}_{k=t+1}^{t+T}$ along each path τ_e and denote $Z_k^s(\tau_e)$ to be the observation of spot s at time k when the ego follows path τ_e . Then, we recursively update beliefs $b_k^s(\tau_e)$ using the update rule (16) and the new simulated observations $Z_k^s(\tau_e)$ for each path τ_e . The total information gain of path τ_e for all parking spots is defined to be the entropy reduction from following the path:

$$\mathcal{I}(\tau_e) = \sum_{i=1}^{N_p} (\mathcal{H}(b_t^{s_i}(\tau_e)) - \mathcal{H}(b_{t+N_e}^{s_i}(\tau_e))), \quad (26)$$

where N_e is the length of path $\tau_e = \{x(k)\}_{k=t}^{t+N_e}$. To balance exploration with motion efficiency, we use (18) and (26) to define the exploration cost

$$\mathcal{C}_e(\tau_e) = \mathcal{C}(\tau_e) - \mathcal{I}(\tau_e), \quad (27)$$

and select the optimal path as $\arg \min_{\tau_e \in \mathcal{T}'} \mathcal{C}_e(\tau_e)$, subject to safety thresholds. If no safe path exists, a backup planner keeps the vehicle stationary or steers it away from adversarial dynamic agents on a collision course.

V. EXPERIMENTAL RESULTS

The task for the ego vehicle is to navigate from the initial position to a feasible parking spot, assuming that the onboard sensors provide real-time information on static vehicles, driving aisles and dynamic agents within the FoV. We evaluate our framework in a simulated parking lot environment designed to emulate a shopping mall layout as shown in Fig. 1. The mall entrance is located at the top edge, centered along the x -axis. To reflect realistic congestion patterns, the initial occupancy probability of each parking spot is randomized using a binomial distribution, with higher occupancy near the entrance and lower occupancy farther away as presented in Fig. 3. For evaluation, we conduct ablation studies and baseline comparisons with existing valet parking approaches, and compute key performance metrics in Table III. We run 50 randomized experiments for each method in Table III, randomizing the parking lot configuration, ego vehicle's initial position, and the behavior of other dynamic agents. The ego vehicle is initialized either inside a parking row or outside, while other vehicles may start inside vacant spots or outside. The paths of other vehicles are generated using a local Hybrid A star planner for each vehicle entering or exiting a spot. Dynamic pedestrians are spawned randomly outside parking spots and move with velocities $v \sim \mathcal{U}[-1.5, 1.5]$ m/s. All simulations are performed in Python 3.13 on Ubuntu 20.04 with Intel Xeon E5-2643 v4 CPU.

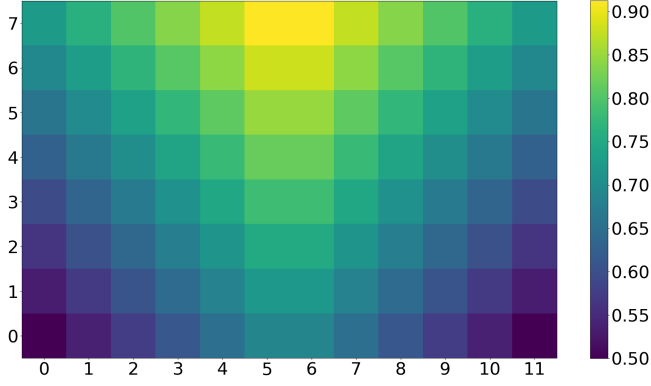


Fig. 3: Initial occupancy probabilities for the parking lot in Fig. 1, consisting of 8 rows and 12 columns of spots.

Simulation parameters: The vehicle dynamics are modeled using the kinematic bicycle model (1), discretized with a time step of 0.1 s for simulation. The vehicle parameters are listed in Table I, based on the 2024 Honda Accord [17]. Our Hybrid A* planner employs a state grid resolution of 2 m in both X and Y directions, and 10 deg for heading. The steering input is discretized into 5 values over $[-\delta_{\max}, \delta_{\max}]$, while velocity is discretized into 5 values over $[-v_{\max}, v_{\max}]$. Parking lot parameters are adopted from [18] and given in Table II. We use a prediction horizon of $T = 5$ s for our spot occupancy estimator and a maximum wait time of $T_w = 5$ s in our strategy planner. The arrival rate λ_a is 0.000624 (14), while the departure rate λ_d is 0.000378 (12), both of which are obtained from the parking lot data in [19]. The probability thresholds in (17) are $P_v = 0.3$ and $P_o = 0.7$. The scaling factor is $r = [(2.5V_L)^{-1} \quad (3V_W)^{-1}]^T$ and forward shift is $\zeta = 0.5V_L$ in (2), while $\eta = 0.5$ in (23). The observability thresholds are $\epsilon = 1$ and $\gamma = 1.5$.

TABLE I: Vehicle parameters

Parameter	Value	Parameter	Value
Length V_L	4.97 m	Spot length	6.1 m
Width V_W	1.86 m	Spot width	2.74 m
Wheelbase L	2.83 m	Road width l_w	7.62 m
Speed limit v_{\max}	3.5 m/s		
Steering limit δ_{\max}	34.9 deg		

TABLE II: Parking lot parameters

A. Ablation Studies

We assess our different contributions by performing ablation studies on the spot occupancy estimator and strategy planner separately. In each case, we fix a specific module and vary components of the other, comparing simplified variants against our proposed design.

1) *Spot Occupancy Estimator:* We fix our strategy planner (Section IV) and compare the performance of three different spot occupancy estimators with ours (Section III).

- **Greedy** approach assumes a horizon of $T = 1$ in the belief estimation equations in Section III, thereby relying only on the instantaneous occupancy probabilities.

- **Identical prediction** method applies the same prediction equation (11) regardless of whether a spot is initially vacant or occupied.
- **Position only** approach models dynamic agents without incorporating velocity by removing the alignment factor (8) in (6) so that $p(s, j, k) = E_d$.

In Fig. 4, we compare our estimator with the Greedy and Identical prediction method. The Greedy approach uses only the current occupancy, while ours predicts over a horizon by modeling vacant and occupied dynamics separately. Hence, our estimator significantly lowers the occupancy probability when a vehicle departs, unlike the Identical prediction (Fig. 4e). This yields a parking time of 11.5 s for our approach, compared to 16.5 s for others. Moreover, when the red vehicle briefly passes near the vacant spot V, its occupancy probability momentarily increases but later decreases since we incorporate velocity ((6) and (8)), whereas the probability for the initially occupied spot steadily decreases. Although spot V remains vacant, the planner avoids it since it is surrounded by static vehicles and selects a more accessible spot.

In Fig. 5, we compare our estimator with the Position only method as a vehicle passes a vacant spot. The Position only method assigns a higher occupancy probability to the spot (Fig. 5b), incorrectly classifying the spot to be occupied from (17) ($P_v = 0.3$). This misclassification leads the ego to skip the spot, resulting in longer parking times and less smooth trajectories (Fig. 5c). The ego hence performs a backup maneuver before briefly waiting for a pedestrian crossing the road, who was initially outside the FoV (Fig. 5a).

2) *Strategy Planner:* We fix the spot occupancy estimator (Section III) and compare two strategy planner variants against ours (Section IV):

- **No wait time** always sets $t_w = 0$ in (18) so that it never

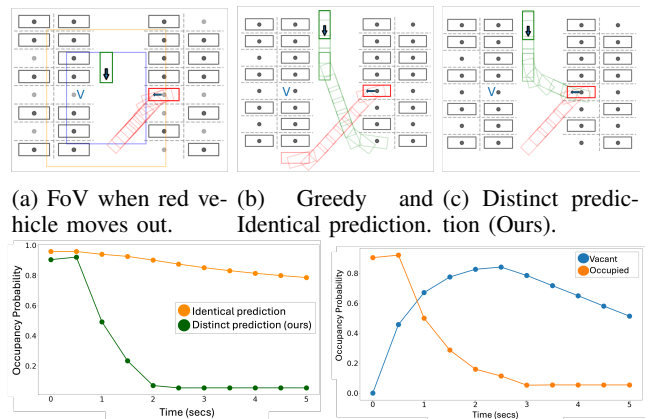


Fig. 4: Comparison of ego vehicle (green) trajectories and occupancy probabilities when a vehicle (red) vacates a spot with a nearby vacant spot (V). The Greedy and Identical estimators require 16.5 s to park, while our approach completes the maneuver in 11.5 s.

pauses near a potentially vacant spot.

- **Lawn-mower** performs pure exploration ($\mathcal{C}_e(\tau_e) = -\mathcal{I}(\tau_e)$ in (27)) when no promising spots are available as classified by (17).

Fig. 6 compares the no wait time strategy with ours. Although the spot occupancy estimator predicts the initially occupied spot to be vacant in the future as illustrated in Fig. 4d, the no wait strategy cannot plan a safe path and instead explores further before backing up, resulting in longer parking times. Our planner balances the trade-off between waiting and exploring, enabling the ego to park in an initially occupied spot (Fig. 6c) by permitting short, bounded waits. This behavior is especially valuable in dynamic environments where briefly waiting near a nearly vacant spot is more

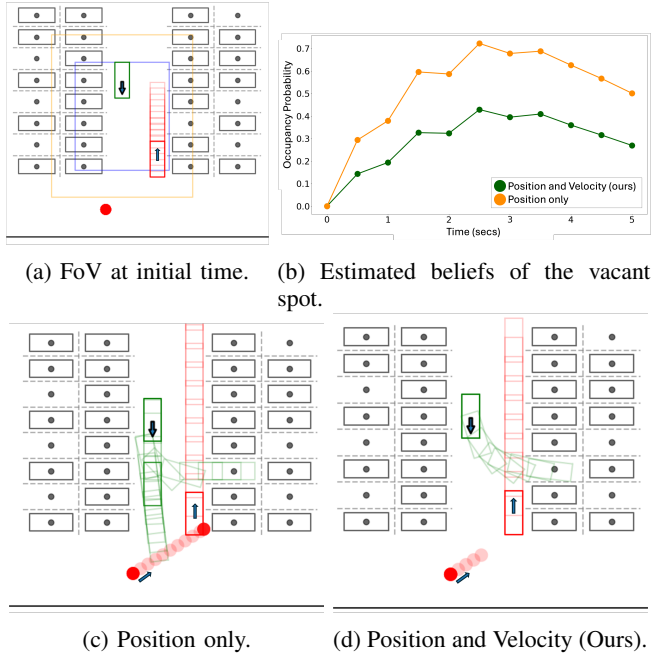


Fig. 5: Comparison of ego vehicle (green) trajectories and occupancy probabilities when a vehicle (red rectangle) passes a vacant and a pedestrian is entering another vehicle (red circle). The Position only method require 24 s to park, while our approach completes the maneuver in 11 s.

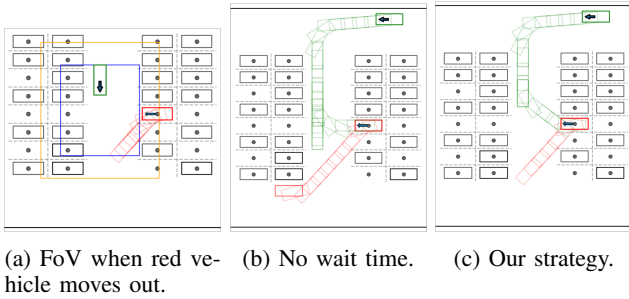


Fig. 6: Comparison of ego vehicle (green) trajectories when there is no wait time in (18) and another vehicle (red) moves out of a spot. The No wait time strategy requires 27 s to park, while our strategy completes parking in 18 s.

efficient than abandoning it.

In Fig. 7, we show an example where the lawn-mower strategy wastes time exploring a crowded row despite feasible spots present in the adjacent row. Since it is purely exploration driven, the ego must wait for other vehicles both at the row entrance and inside, leading to larger parking time (Fig. 7b). Our strategy planner balances exploring the lot and exploiting smoother paths (Fig. 7c), thus avoiding costly detours and achieving shorter parking times.

B. Comparison with Existing Work

We benchmark our integrated spot occupancy estimator and strategy planner against three existing valet parking approaches: *InfPath - Traversal* [6], *InfPath - MCBFT* [6] and *Rule-OBCA* [8]. The *InfPath* method uses a Vanilla Bayes filter to estimate spot occupancies with a FoV observation model independent of distance from ego vehicle, and presents two planning methods: Traversal (Section IV-B of [6]) and Monte Carlo Bayes Filter Tree (MCBFT) (Section IV-C of [6]). While [6] is originally designed for exploration without dynamic obstacle avoidance, we apply our safety thresholds to discard unsafe paths and park at the closest available spot within the FoV.

- **InfPath - Traversal** samples all feasible paths over a planning horizon of $T = 5$ secs, and selects the one that either parks at the closest spot or maximizes the information gain with obstacle avoidance. Information gain is computed using the occupancy estimation method presented in Section III of [6].
- **InfPath - MCBFT** builds a policy tree from spot occupancy probabilities and selects paths using the Upper Confidence Bound.
- **Rule-OBCA** chooses the closest available spot within the FoV and plans via rule-based dynamic collision avoidance with Model Predictive Control, using smooth nonlinear obstacle avoidance constraints [4].

Quantitatively, Table III shows that our approach substantially improves key planning metrics over existing approaches [6], [8] and variations of our approach (Section V-A), reducing path length and parking time while achieving lower smoothness costs and greater clearance from obstacles, resulting in more efficient and safer parking maneuvers.

VI. CONCLUSION AND FUTURE WORK

We present a trajectory planning framework for autonomous valet parking that integrates a novel *spot occupancy estimator* and a *strategy planner* for uncertain, dynamic environments with limited FoV. The occupancy estimator distinguishes initially vacant and occupied spots to estimate future occupancy probabilities, while also incorporating motion of dynamic agents. This estimator is integrated with our strategy planner that balances information gain with goal-directed planning, and employs wait-and-go behaviors for promising spots. Simulation results show that our method outperforms existing approaches in efficiency, safety, and smoothness.

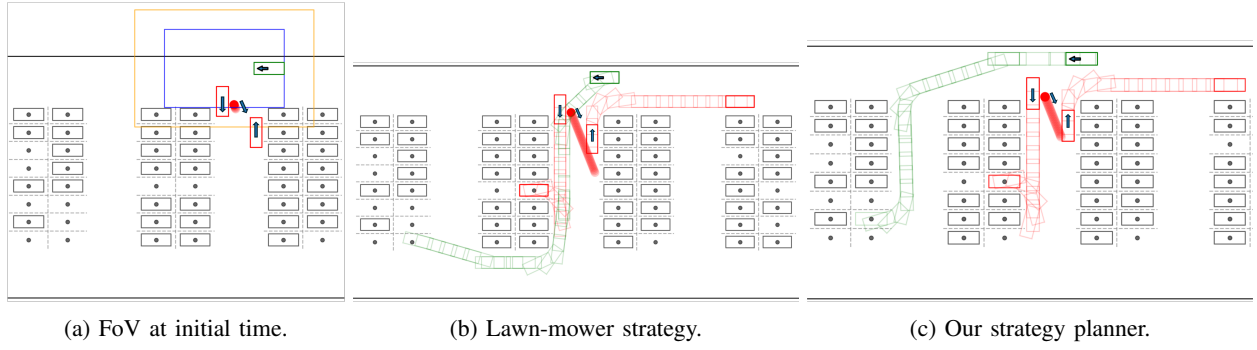


Fig. 7: Comparison of trajectories when the ego vehicle (green) is initially outside the row of parking spots and a row is crowded with other dynamic agents (red). The lawn-mower strategy requires 43.5 s to park, while our strategy completes parking in 25.5 s.

TABLE III: Planning metrics for 50 randomized experiments across different methods: ablation studies in **spot occupancy estimator** and **strategy planner**, and **existing work**. The numbers in **green** denote the best value for each metric.

Method	Runtime ↓ (s)	Path length ↓ (m)	Parking time ↓ (s)	Average distance to closest dynamic obstacle ↑ (m)	Minimum distance to closest static obstacle ↑ (m)	Smoothness cost ↓	Average heading rate ↓ (deg/s)	Average curva- ture ↓ (m^{-1})
Greedy	0.041 ± 0.002	34.603 ± 3.113	23.702 ± 5.211	3.335 ± 0.103	0.315 ± 0.041	4.655 ± 2.83	12.995 ± 2.341	0.061 ± 0.02
Identical prediction	0.051 ± 0.002	32.589 ± 2.773	22.575 ± 4.097	3.687 ± 0.074	0.278 ± 0.092	4.302 ± 1.12	12.16 ± 1.154	0.056 ± 0.002
Position only	0.049 ± 0.008	33.735 ± 5.298	21.539 ± 1.359	8.331 ± 0.949	0.314 ± 0.131	5.045 ± 2.45	14.6 ± 2.881	0.058 ± 0.012
No wait time	0.065 ± 0.002	45.735 ± 5.328	28.524 ± 2.533	9.228 ± 1.25	0.264 ± 0.066	32.668 ± 4.987	18.989 ± 3.1	0.058 ± 0.015
Lawn-mower	0.127 ± 0.03	41.858 ± 3.37	32.532 ± 3.58	3.273 ± 0.119	0.273 ± 0.013	12.536 ± 3.1	17.032 ± 1.725	0.059 ± 0.008
InfPath - Traversal	0.059 ± 0.001	42.364 ± 3.15	26.725 ± 5.71	5.232 ± 0.579	0.261 ± 0.078	13.583 ± 1.541	16.86 ± 2.97	0.061 ± 0.034
InfPath - MCBFT	0.281 ± 0.012	35.742 ± 2.05	23.35 ± 2.13	6.634 ± 1.02	0.276 ± 0.044	14.543 ± 2.146	14.655 ± 2.51	0.077 ± 0.009
Rule-OBCA	0.416 ± 0.055	32.94 ± 2.11	25.195 ± 2.54	9.376 ± 0.974	0.335 ± 0.095	20.54 ± 1.981	15.375 ± 1.632	0.062 ± 0.04
Ours	0.045 ± 0.005	24.001 ± 2.992	17.179 ± 4.333	8.564 ± 1.03	0.271 ± 0.052	3.513 ± 0.95	11.119 ± 2.2	0.024 ± 0.002

The following limitations in our work suggest directions for future work. First, our Hybrid A star planner limits control diversity. Hence, exploring sampling-based methods like MPPI [13] could enable richer strategies under tight constraints. Second, incorporating intent inference (e.g., parking, yielding, exiting) of other agents for interaction-aware planning could improve realism and safety. Third, integrating occlusion-aware sensing models could provide more realistic occupancy estimates. Finally, developing adaptive waiting behaviors by varying the maximum waiting time could lead to more efficient parking in dense parking lots.

REFERENCES

- [1] Tesla Model 3 Owner’s Manual, 2024. [Online].
- [2] Kathryn Tomczak, Adam Pelter, Corey Gutierrez, Thomas Stretch, Daniel Hilf, Bianca Donadio, Nathan L. Tenhundfeld, Ewart J. de Visser, and Chad C. Tossell. Let tesla park your tesla: Driver trust in a semi-automated car. In *2019 Systems and Information Engineering Design Symposium (SIEDS)*, pages 1–6, 2019.
- [3] International Organization for Standardization. Intelligent transport systems — Automated valet parking systems (AVPS) — Part 1: System framework, requirements for automated driving and for communications interface, 2023.
- [4] Xiaojing Zhang, Alexander Liniger, and Francesco Borrelli. Optimization-based collision avoidance. *IEEE Transactions on Control Systems Technology*, 29(3):972–983, 2020.
- [5] Xu Shen, Edward L Zhu, Yvonne R Stürz, and Francesco Borrelli. Collision avoidance in tightly-constrained environments without coordination: a hierarchical control approach. In *2021 IEEE International Conference on Robotics and Automation (ICRA)*, pages 2674–2680. IEEE, 2021.
- [6] Yunze Hu, Jiaao Chen, Kangjie Zhou, Han Gao, Yutong Li, and Chang Liu. Informative path planning of autonomous vehicle for parking occupancy estimation. In *2023 IEEE 26th International Conference on Intelligent Transportation Systems (ITSC)*, pages 3304–3310. IEEE, 2023.
- [7] Jean-Luc Lupien, Abdullah Alhadlaq, Yuhan Tang, Jiayu Joyce Chen, and Yutan Long. Entropy-based dynamic programming for efficient vehicle parking. *arXiv preprint arXiv:2411.17014*, 2024.
- [8] Xu Shen, Yongkeun Choi, Alex Wong, Francesco Borrelli, Scott Moura, and Soomin Woo. Parking of connected automated vehicles: Vehicle control, parking assignment, and multi-agent simulation. *arXiv*

preprint arXiv:2402.14183, 2024.

- [9] Farhad Nawaz, Minjun Sung, Darshan Gadginmath, Jovin D'sa, Sangjae Bae, David Isele, Nadia Figueroa, Nikolai Matni, and Faizan M Tariq. Graph-based path planning with dynamic obstacle avoidance for autonomous parking. *arXiv preprint arXiv:2504.12616*, 2025.
- [10] Rajesh Rajamani. *Vehicle dynamics and control*. Springer Science & Business Media, 2011.
- [11] Sebastian Thrun, Wolfram Burgard, and Dieter Fox. *Probabilistic Robotics (Intelligent Robotics and Autonomous Agents)*. The MIT Press, 2005.
- [12] Mahalanobis Prasanta Chandra et al. On the generalised distance in statistics. In *Proceedings of the National Institute of Sciences of India*, volume 2, pages 49–55, 1936.
- [13] Francesca Baldini, Faizan M. Tariq, Sangjae Bae, and David Isele. Don't get stuck: A deadlock recovery approach. In *2024 IEEE 27th International Conference on Intelligent Transportation Systems (ITSC)*, pages 3688–3695, 2024.
- [14] Wenda Xu, Qian Wang, and John M Dolan. Autonomous vehicle motion planning via recurrent spline optimization. In *2021 IEEE International Conference on Robotics and Automation (ICRA)*, pages 7730–7736. IEEE, 2021.
- [15] Wolfram Research. CosineDistance. <https://reference.wolfram.com/language/ref/CosineDistance.html>, 2007.
- [16] Sangjae Bae, David Isele, Alireza Nakhaei, Peng Xu, Alexandre Miranda Añon, Chiho Choi, Kikuo Fujimura, and Scott Moura. Lane-change in dense traffic with model predictive control and neural networks. *IEEE Transactions on Control Systems Technology*, 31(2):646–659, 2022.
- [17] 2024 Honda Accord Specifications and Features , 2023. [Online].
- [18] La Puente, CA, Municipal Code §10.30.070 “Parking Space and Drive Aisle Dimensions”, 2024. [Online].
- [19] Jun Xiao, Yingyan Lou, and Joshua Frisby. How likely am i to find parking?—a practical model-based framework for predicting parking availability. *Transportation Research Part B: Methodological*, 112:19–39, 2018.

APPENDIX

Uncertainty Propagation: We propagate the positional covariance at each timestep using a standard discrete-time model. The covariance matrix $\Sigma(k)$ is updated as

$$\Sigma(k+1) = R(\theta(k)) (\Sigma(k) + Q) R(\theta(k))^{\top},$$

where $R(\theta(k))$ is the rotation matrix parameterized by the vehicle's heading $\theta(k)$ and Q is a diagonal matrix representing the process noise in the local frame. The initial covariance is $\Sigma(t) = \begin{bmatrix} \beta_l L & 0 \\ 0 & \beta_w W \end{bmatrix}$, with L and W denoting the length and width of the vehicle, while β_l and β_w correspond to the respective scaling factors. If the dynamic agent is a pedestrian, then $\theta(k) = 0$ deg, $\beta_l = \beta_w = 1$, and we use a radius parameter to represent the size of the pedestrian instead of the length and width of the vehicle. To estimate the uncertainty in velocity, we approximate the instantaneous velocity as the finite difference $v^j(k) = \frac{y^j(k+1) - y^j(k)}{\Delta t}$, where Δt is the time interval between successive time steps. The resulting covariance in velocity is

$$\Sigma_v(k) = \frac{\Sigma(k+1) + \Sigma(k) - 2\Sigma_{\rho}}{\Delta t^2},$$

where $\Sigma_{\rho} = \text{Cov}(y^j(k+1), y^j(k))$ models the covariance between consecutive position estimates. We assume a symmetric form and set $\Sigma_{\rho} = \begin{bmatrix} \rho & 0 \\ 0 & \rho \end{bmatrix}$ for all $j \in \{1, 2, \dots, D\}$ and $k \in \{t, t+1, \dots, t+T-1\}$. Note that when $\rho \neq 0$, the velocity estimate is not Gaussian since sum of two Gaussian

random variables is a Gaussian only if they are independent (uncorrelated) or jointly Gaussian.